Study of Component Aerosol Direct Radiative Effect over the Asian Region

Tom X.-P. Zhao

National Climate Data Center, NOAA/NESDIS, Asheville, NC 28801, USA & ESSIC, University of Maryland, College Park, MD20743
E-mail: xuepeng.zhao@noaa.gov

Abstract
A two-step approach of combing CERES/MODIS shortwave (SW) flux and aerosol optical thickness (AOT) at 0.55μm with the component AOT fractions from a 3-D aerosol model is used to derive top of atmosphere (TOA) component aerosol direct radiative effect (ADRE) over the Asian region for the clear-sky condition. The annual mean values of ADRE for the region are +0.55±0.1W/m² for black carbon (BC); -1.23±0.39W/m² for organic carbon (OC); -3.81±0.71W/m² for sulphate (SU); -3.16±0.45W/m² for dust (DU); -0.64±0.55W/m² for sea salt (SS); -3.98±0.57W/m² for anthropogenic aerosol (AN); -4.37±1.11W/m² for natural aerosol (NA); and -8.37±1.69W/m² for total aerosols (TOT). Both anthropogenic and natural aerosol direct radiative effects in the region are much higher than their global counterparts. Validations have also been performed by comparing our component ADRE computation with the radiative transfer calculations for the AERONET sites and the ACE-Asia field campaign.
Keywords
aerosol direct radiative effect, aerosol optical thickness

I. INTRODUCTION

Tropospheric aerosols, due to their regional nature, cause the largest uncertainties in assessing the climate forcing of atmospheric constituents associated with anthropogenic activity(IPCC,2007). The excessive amounts of trace gases and aerosol particles have been released into the atmosphere in the Asian region due to the fast development of regional economy during the past three decades. This has caused irreversible changes/damages to the air quality and climate in the Asian region, which becomes a unique area for the study of the effect of modernization on the Earth environment. In this paper, we study aerosol direct radiative effect (ADRE), defined as the effect of both natural and anthropogenic aerosols on the radiative fluxes, in the Asian region. Specifically, we analyze the ADRE for different aerosol components so that the anthropogenic impact can be evaluated. Due to the advance of satellite aerosol measurement in recent years, satellite aerosol observations have been actively used to estimate regional and global ADRE for the ensemble anthropogenic aerosols. However, it is still difficult using satellite observations alone to further derive ADRE for more detailed aerosol components, such as sea salt (SS), dust (DU), sulphate (SU), black carbon (BC) and organic carbon (OC), over a continental region heavily influenced by aerosols with complex chemical and optical properties, such as Asia. Here, we derive top-of-atmosphere (TOA) ADRE for different aerosol components on clear-sky condition over the Asian continent by combing satellite measured shortwave (SW) radiation flux and aerosol optical thickness (AOT) with the component AOT fractions from a 3-D aerosol model.

II. SATELLITE AND MODEL PRODUCTS

We divide aerosols into five externally mixed components: BC, OC, SU, DU, and SS. The total AOT (or τ) is the sum of the five component AOTs ($\tau_{TOT} = \sum_{i=1}^{5} \tau_i$). Moreover, BC, OC, and SU are further grouped as anthropogenic aerosols (AN) after removing the natural organic carbon (OCn) and natural sulphate (SUn). The natural aerosols (NA) are determined by subtracting the AN from the total aerosols. To facilitate the validation using the AERONET observation, we group BC, OC, and SU plus accumulation mode of dust (DUa) and sea salt (SSa) as fine mode (FN) aerosols. Then, the coarse mode aerosols (CR) are determined by subtracting the FN from the total aerosols. The fraction (r_i) of individual component AOT for BC, OC, SU, DU, SS, AN, NA, FN, and CR is determined using the relationship $r_i = \tau_i / \tau_{TOT}$ (i = BC, OC, SU, DU, SS, AN, NA, FN, and CR). The monthly averaged AOT at 0.55μm (or $\tau_{0.55}$) from the Goddard Global Ozone Chemistry Aerosol Radiation and Transport (GOCART) model (Chin M, et al., 2000) is used for the determination of r_i in the current study.

The clear-sky narrow band MODIS radiances are converted to broadband SW radiances by applying a narrow-to-broadband conversion. The converted broadband radiances are used to determine TOA SW fluxes using empirical Angular Distribution Models (ADMs) developed from CERES(Loeb N G, et al., 2005). The TOA SW fluxes are further used to derive TOA ADRE (which is defined as the difference between SW radiative fluxes in absence and presence of aerosol in cloud-free conditions) following the approach used in Loeb and Manalo-Smith(Loeb N G, et al., 2005). The final TOA ADRE product is in 1° × 1° spatial resolution and will be called CERES/MODIS ADRE product hereafter. The MODIS Collection 4 aerosol product (MOD04) is used to determine daily TOA ADRE for year 2001, which is further averaged to obtain monthly mean values with a spatial resolution of 1° × 1°. The

1082-4006/08/14(02)-80$5.00

final monthly averaged AOT (τ_{TOT}) at 0.55μm are partitioned into major aerosol components (τ_i, i=BC, OC, SU, DU, SS, AN, NA, FN, and CR) by using the component fractions (r_i) from the GOCART model with $\tau_i = r_i$(GOCART)×τ_{TOT}(MODIS). The resultant component AOTs from the partitioning are used to derive component ADRE as introduced in the Section III.

Both CERES TOA SW fluxes and MODIS AOTs are used in the following ADRE analysis. Aerosol information is also needed to drive TOA SW fluxes from the observation of satellite CERES instrument. Since CERES and MODIS instruments are on the same EOS satellite platform, the MODIS aerosol products are naturally selected in the CERES data processing for determining CERES TOA SW fluxes. However, there is always a delay for including the newest MODIS products into CERES data processing. We have noticed that MODIS aerosol product has been improved in current Collection 5 compared to the last Collection 4, especially over the land(Li Z, et al., 2007). However, the most recent version of CERES data contains only MODIS Collection 4 aerosol product and Collection 5 aerosol product will be included in the next round of CERES data processing. To avoid inconsistence between the aerosol information used for determine CERES SW fluxes and that used in current partitioning calculation, we decide to still use the MODIS Collection 4 AOT data in current analysis.

III. METHODOLOGY

A two-step approach(T X-P Zhao, et al., 2007) is used for deriving TOA component ADRE for clear-sky condition over the Asian region. The first step is to derive total ADRE and the second step is to partition the total ADRE into each aerosol component. The method used by Loeb and Manalo-Smith (Loeb N G, et al., 2005) is adopted as the first step. The TOA ADRE for a given day (d) and given location at latitude(θ) and longitude(φ) is given by

$$\Delta F(d,\theta,\varphi) = \overline{F}^{na}(d,\theta,\varphi) - \overline{F}^{a}(d,\theta,\varphi) \quad (1)$$

where $\overline{F}^{na}$ and $\overline{F}^{a}$ are the daily averaged TOA upward SW fluxes in the absence and presence of aerosols, respectively. They are determined from instantaneous TOA SW fluxes (F^{na} and F^{a}) in several steps. First, the narrowband clear-sky MODIS radiances are converted to broadband SW radiances (I_{SW}) by applying a three-channel narrow-to-broadband regression conversion. Then, I_{SW} is further used to determine F^{a} with the CERES ADMs. More detailed description can be found in Loeb and Manalo-Smith(Loeb N G, et al., 2005).

Over ocean, F^{na} is inferred from the relationship between SW TOA flux and MODIS $\tau_{0.55}$. In each 1°-interval of solar zenith angle (SZA) where data are available, F^{a} are plotted against $\tau_{0.55}$, and a regression line is fit to the data, the intercept of the regression line—i.e., the TOA flux extrapolated to zero AOT—approximates the mean "no aerosol flux" as a function of SZA. Over land, F^{na} is computed from broadband Fu-Liou radiative transfer model(Fu Q, et al., 1993) calculations for a molecular atmosphere with input surface spectral albedos from the MODIS Filled Land Surface Albedo (FLSA) product (Moody E G, et al., 2005). The instantaneous TOA fluxes ($F^{na}$and F^{a}) then converted to a 24-hour mean TOA fluxes by applying diurnal albedo models to estimate what the reflected SW flux would be at all local times of the day assuming no changes in aerosol or surface properties, and averaging these fluxes over the full 24-hour of local time. The daily averaged ADRE is further averaged to obtain monthly mean TOA total ADRE in 1° × 1° spatial resolution.

The second step is to partition the total ADRE into each aerosol component using the method proposed in Zhao et al.(T X-P Zhao, et al., 2007). For non- or weakly-absorbing components (such as OC, SU, DU, SS, NA, and CR), their direct radiative effect is determined from

$$\Delta F_i(m,\theta,\varphi) = \Delta F(m,\theta,\varphi)\times(e^{-\tau_i}-1)/(e^{-\tau}-1) \quad (i = \text{OC, SU, DU, SS, NA, and CR}) \quad (2)$$

where m indicates monthly mean. For strong absorbing BC, its ADRE is obtained by subtracting the ADRE of OC, SU, DU, and SS from the total ADRE. For absorbing AN or FN component, their ADRE is determined by subtracting the NA or CR ADRE from the total ADRE according to

$$\Delta F_{AN\text{ or }FN}(m,\theta,\varphi) = \Delta F(m,\theta,\varphi) - \Delta F_{NA\text{ or }CR}(m,\theta,\varphi) \quad (3)$$

In the current study, the analysis is confined to the Asian region (10°N–50°N; 50°E–150°E) and year 2001 and our focus is on the examination of seasonal and annual mean distributions of component ADRE for the region.

IV. RESULTS

Figure 1 displays the distribution of annual mean ADRE and the corresponding AOT for the Asian region. Strong negative ADRE is observed over the eastern and north-western China, south-east Asia, the Arabian Sea, and the northern India in Figure 1(b). These patterns are consistent with those of AOT distribution shown in Figure 1(a). The regional annual mean AOT/ADRE of total aerosols is 0.343/–8.374 (W/m^2).

Figure 2 plots the distributions of annual mean ADRE and AOT for the anthropogenic and natural aerosol components. The anthropogenic aerosols are mainly located over the eastern China, south-east Asia, and the northern India and strong negative ADRE is also observed in these areas. The natural aerosols are mainly located in the north-western China and the Arabian Sea and produce a strong negative ADRE accordingly. The regional annual mean AOT/ADRE of AN and NA is 0.165/–3.985 (W/m^2) and 0.177/–4.373 (W/m^2), respectively.

Figure 3 further displays the distribution of TOA ADRE for BC, OC, SU, DU, SS, and total aerosols. The strong negative ADRE over the eastern China (see Figure 3(a)) is mainly due to the contribution of sulfate (Figure 3(f)). The negative ADRE over the south-east Asia and the northern India is mainly from the contribution of SU and OC. The strong negative ADRE over the Arabian Sea is due to the contributions of

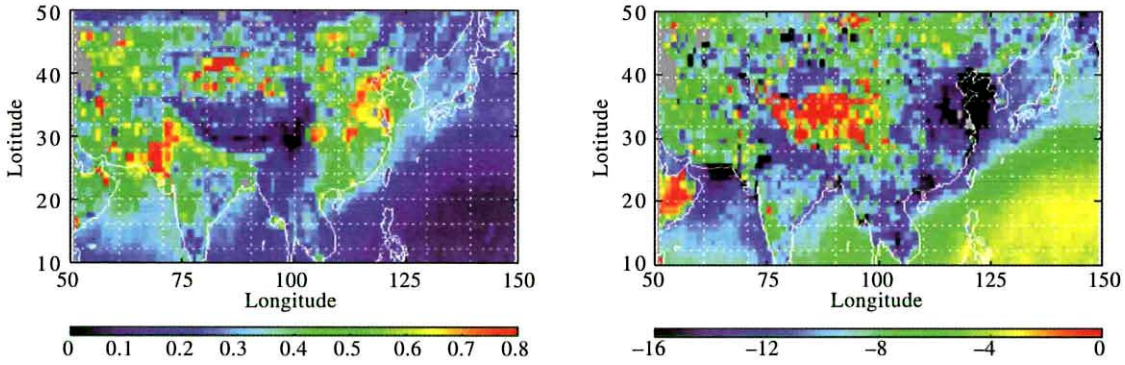

(a) AOT at 0.55μm, 2001 (b) TOA total ADRE (W/m²), 2001

Figure 1. Distributions of 2001 annual mean

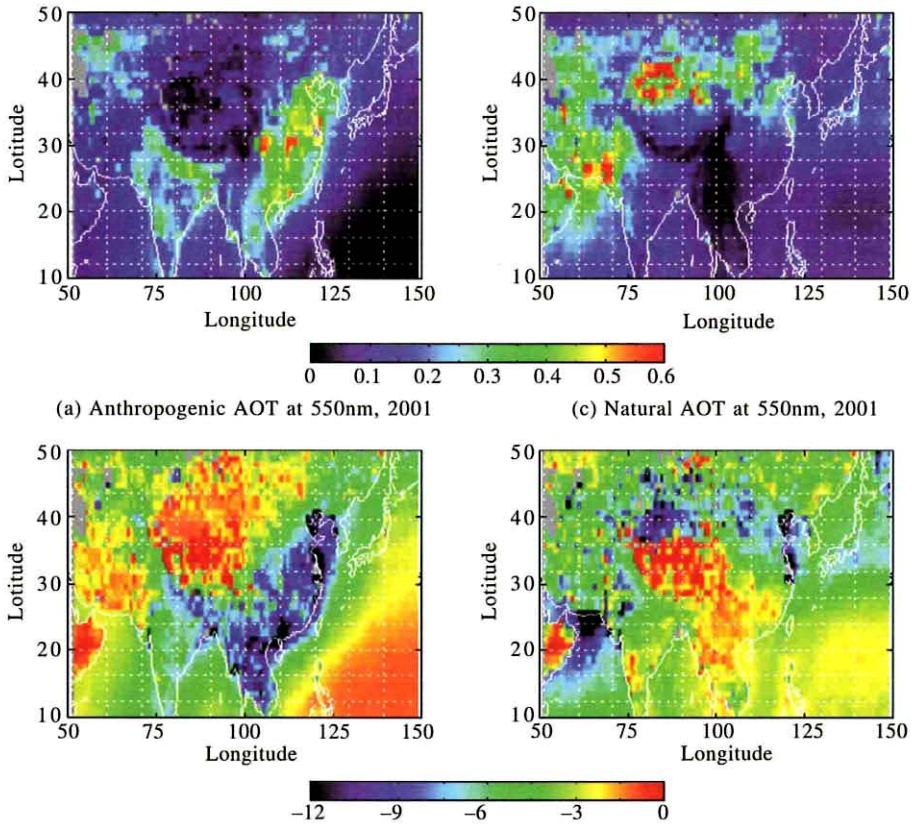

(a) Anthropogenic AOT at 550nm, 2001 (c) Natural AOT at 550nm, 2001

(b) Anthropogenic ADRE(W/m²), 2001 (d) Natural ADRE(W/m²), 2001

Figure 2. Distribution of annual mean AOT at 0.55μm ((a) & (c)) and TOA ADRE ((b) & (d)) for the anthropogenic (AN) and natural (NA) aerosol components

DU, SU, OC, and SS. The negative ADRE over the north-western China is from the contribution of DU. ADRE of BC is positive and the highest values are located in the Arabian Sea, the north-eastern China, and the northern India. The regional annual mean AOT/ADRE of BC, OC, SU, DU, SS, and total aerosols is 0.018/+0.549 (W/m²), 0.039/–1.230 (W/m²), 0.130/–3.808 (W/m²), 0.137/–3.157 (W/m²), 0.019/–0.644 (W/m²), and 0.343/–8.374 (W/m²), respectively.

The seasonal and annual mean values of TOA component ADRE is shown in Figure 4. ADRE of BC, OC, DU, SU, and total aerosol is strongest in Spring (MAM). BC, SU, and total aerosols show a minimal ADRE in Fall (SON) while ADRE of OC reaches minimum in Summer (JJA). ADRE of SU and SS show very minor seasonal change but ADRE of DU shows strong seasonal changes. These season variations of component ADRE are consistent with the seasonal variations of aerosol loading (AOT) and emissions (Streets D G, et al., 2003).

V. VALIDATION

Both surface AERONET observations and field campaign measurement are used to validate our results.

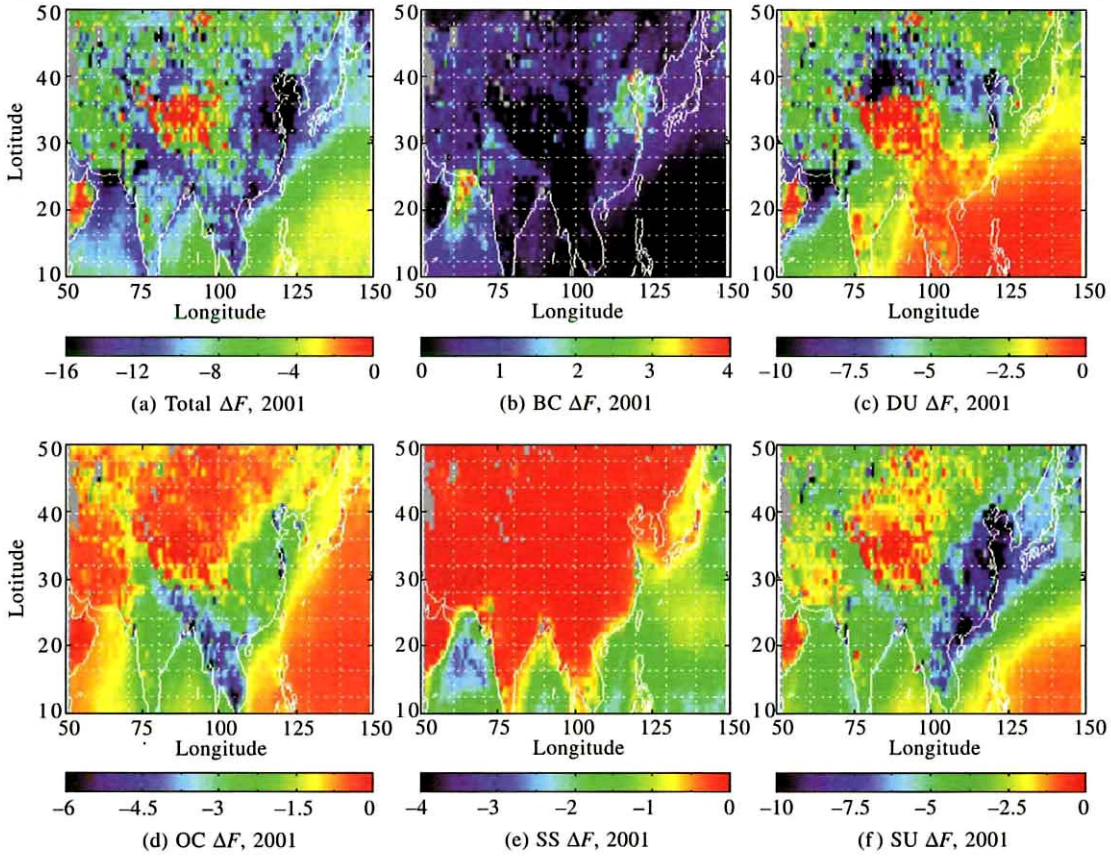

Figure 3. Distribution of annual mean TOA ADRE

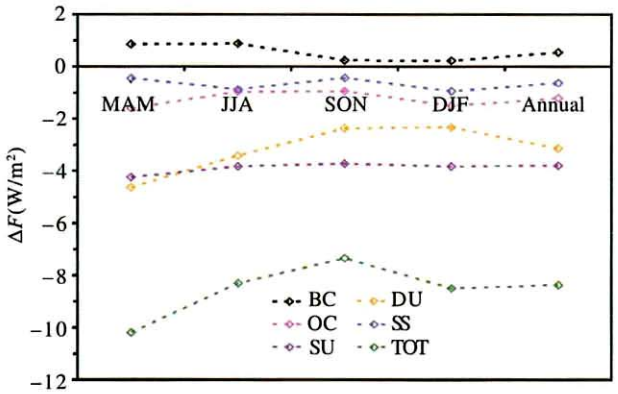

Figure 4. Seasonal and annual mean values of TOA component ADRE

A. AERONET observation

A Fu-Liou radiative transfer model(Fu Q, et al., 1993) is used to calculate the monthly mean TOA ADRE over the AERONET sites by using aerosol optical properties (including AOT, single scattering albedo, asymmetry factor, and size distribution) observed from AERONET and surface reflectance(Moody E G, et al., 2005) obtained from MODIS observations as inputs for the model. The monthly mean ADRE computation for the AERONET sites is performed not only for total aerosols but also for fine and coarse mode aerosols if their optical properties are available from the AERONET observations. This radiative transfer calculation is considered as the reference for our validation. According to Zhou et al.(Zhou M, et al., 2005), three AERONET sites (Anmyon, NCU_Taiwan, and Shirahama) have been selected over the East Asia for the radiative transfer calculation due to their long temporal coverage and high quality. Please refer to Zhou et al. (Zhou M, et al., 2005) for a detailed description on the selection of AERONET sites and the radiative transfer calculation. We select monthly aerosol climatology from the AERONET observation over the eastern Asia, which is influenced mainly by the fine model aerosols of the pollution. A window of ±2° latitude/longitude around each AERONET site is used for sampling the monthly mean TOA CERES/MODIS ADRE and the averaged value for the window is compared with the radiative transfer calculation for the site. Specifically, the probability distribution functions (PDF) of ADRE from the reference radiative transfer calculation and the CERES/MODIS calculation for the AERONET sites are compared to examine the statistical agreement between the two approaches. The ensemble PDF of ADRE from the radiative transfer calculation over the three AERONET sites are compared with the CERES/MODIS calculation in Figure 5 for the FN mode component, which is the dominant component over the region. The plot is generated from 32 monthly match-ups between the two calculations over the three AERONET sites. The mean difference, RMS difference, and mode difference between the two PDFs are 0.69, 2.82, and 0.0 (W/m^2), respectively. The correlation of a linear regression for the match-ups between the two calculations is 72% and

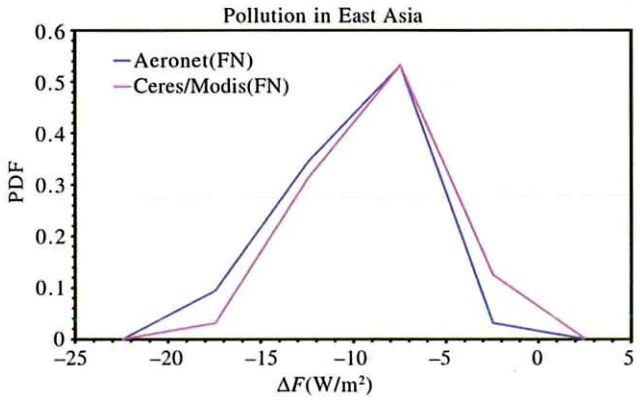

Figure 5. Comparison of the PDF of ADRE of fine mode (FN) aerosols from the radiative transfer calculation based on the AERONET observations with the CERES/MODIS calculation over the ensemble AERONET sites in the East Asia

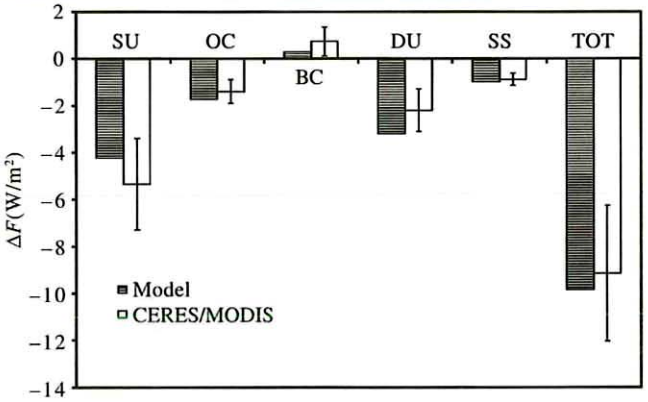

Figure 6. Comparison of TOA component ADRE from a radiation model calculation(Conant, B. C., et al., 2003) with that from the CERES/MODIS computation over the period 5–15 April 2001 during the ACE-Asia Campaign for the oceanic area in the domain of 20°–50°N; 100°–150°E. ±spatial standard error of the CERES/MODIS values is displayed with the vertical error bars. The total ADRE of the model is the simple summation of the individual components

associated standard error is 0.1W/m². The good agreement in the ADRE PDF and linear regression for FN aerosols between the two calculations suggests the partitioning approach introduced in Section III for deriving component ADRE works very well in the Asian region.

B. Field Campaigns

The Asian Pacific Regional Aerosol Characterization Experiment (ACE-Asia) performed in late March through May 2001 over the East Asia and the Northwest Pacific was to determine and understand the properties and controlling factors of the aerosol in the anthropogenically modified atmosphere of the East Asia and the Northwest Pacific and to assess their relevance for radiative forcing of climate (Huebert B J, et al., 2003). The compilation of the data from the observations and model calculations for the experiment can also be used to verify our partitioning calculation for the ACE-Asia region.

A column multiple-scattering Monte Carlo radiation model was developed based on the compilation of the microphysical, chemical, optical, and lidar data during the ACE-Asia(Conant B C, et al., 2003). For a region of 100°E–150°E, 20°N–50°N, this model was used to calculate the averaged component ADRE over the time period 5–15 April 2001 for the mean meteorological and aerosol profiles. The model values averaged over the oceanic area in the domain are compared with our CERES/MODIS computation in Figure 6. The ADRE partitioning tendency of the model calculation and the CERES/MODIS computation is consistent with SU contributes the most followed by DU, OC, SS, and BC, respectively. The difference of individual component ADRE between the Monte Carlo radiation model calculation and the CERES/MODIS computation are within the standard error of the CERES/MODIS component ADRE.

VI. DISCUSSION AND SUMMARY

There are some uncertainties in our estimation of TOA component ADRE due to several error sources. The first error source is associated with the TOA SW clear-sky fluxes, which includes three contributors: uncertainties in the conversion of clear-sky MODIS radiances to broadband SW radiances; uncertainties in the radiance-to-flux conversion (or ADM model); and uncertainties due to cloud contamination. The second error source is the uncertainty associated with the derivation of F^{na}. Their contribution to the uncertainty of TOA total ADRE from the CERES/MODIS observation is about ~1.69 (W/m²) or 24.7% of the total ADRE(T X-P Zhao, et al., 2007). There are also two major error sources for the TOA component ADRE. The first is the error inherited from TOA total ADRE discussed above. We assume the 24.7% relative uncertainty in the TOA total ADRE is propagated equally into individual components. The second error source associated with the TOA component ADRE is the partitioning uncertainty introduced in Section 3 for individual aerosol components. According to Zhao et al.(2007), the partitioning uncertainty is at least 0.080W/m² for BC and 0.312, 0.409, 0.233, 0.136, 0.055, and 0.107 (W/m²) for OC, SU, DU, SS, AN, and NA, respectively. If we assume they are independent from the uncertainty inherited from the total ADRE, the final uncertainties associated with our approach for determining component ADRE should be 0.10, 0.39, 0.71, 0.45, 0.55, 0.57, 1.11, and 1.69 (W/m²) for BC, OC, SU, DU, SS, AN, NA, and total aerosols, respectively. The annual mean values of ADRE over the Asian region are +0.55W/m² for black carbon; –1.23W/m² for organic carbon; –3.81W/m² for sulphate; –3.16W/m² for dust; –0.64W/m² for sea salt; –3.98W/m² for anthropogenic aerosol; –4.37W/m² for natural aerosol; and –8.37W/m² for total aerosols. They are much higher than their global counterparts, +0.25W/m² (BC), –0.97W/m² (OC), –2.32W/m² (SU), –1.57W/m² (DU), –2.16W/m² (SS), –2.38W/m²(AN), –4.46W/m² (NA), and –6.84W/m² (TOT), derived over the globe by using the same approach (Zhao T X-P, et al., 2008). These results are evidence to the damages/changes on the air quality and climate in the Asian region due to excessive industrial emissions associated with the

fast development of regional economy during the past three decades.

The development of global aerosol models is now at a stage that simulated global annual mean AOT value is not only in good agreement with each other but also in good agreement with AERONET observations(Kinne S, et al., 2006). However, there are still large differences in component aerosol optical thickness simulated by different global aerosol models(Kinne S, et al., 2006; Textor C, et al., 2006), especially for natural component (SS and DU) due to their various emission inventories. Our analysis is not immune from this uncertainty in the component aerosol optical thicknesses associated with model simulations, which needs to be improved gradually along with the advancement of global aerosol modeling. The GOCART model AOT simulation is one of the models that compare best with the surface AERONET observation(Kinne S, et al., 2006). Its performance has also been well documented in the literature(Chin M, et al., 2002; Chin M, et al., 2004) and interested readers can refer to the references for more detailed information. Detailed discussions for the possible influence of GOCART model uncertainties on the estimate of ADRE from the two-step approach can be found in a previous work of Zhao et al.(T X-P Zhao, et al., 2007).

The final uncertainties in the component ADRE might be larger than our current estimates since our analysis is directly influenced by the uncertainty in the GOCART model simulation of major aerosol components associated with the current state of global aerosol modelling. To further narrow the uncertainties in the estimation of regional and global component ADRE in the future, an integration of multivariate and multidimensional information from diverse satellite sensors, ground-based instruments, and models is necessary

ACKNOWLEDGEMENTS

The author would like to acknowledge the collaboration with Dr. Norman Loeb at NASA Langley, Dr. Istvan Laszlo at NOAA/NESDIS, and Dr. Mi Zhou at I. M. System Group, Inc. Thanks also go to the NASA CERES project for providing the CERES/MODIS data and Dr. Mian Chin at GSFC for providing the GOCART model data. The comments from one anonymous reviewer are greatly appreciated. The author also would like to acknowledge the great effort of Dr. Long Chiu at the Chinese University of Hong Kong for organizing the JGIS special issue on GCEAP. The work presented in the paper is funded by the NASA Radiation Program managed by Dr. Hal Maring through grant RSP-0022-0005 and the Cooperative Institute Program of NOAA/NESDIS/STAR.

REFERENCES

[1] IPCC, Climate Change, 2007, The Physical Science Basis, New York: Cambridge Univ. Press, pp. 996.

[2] Chin, M., R. B. Rood, S.-J. Lin, J.-F. Muller, Thompson, A. M., 2000, Atmospheric sulfur cycle simulated in the global model GOCART: Model description and global properties, J. Geophys. Res., 105, 24,671-24,687.

[3] Loeb, N. G., S. Kato, K. Loukachine, N. M. Smith, 2005, Angular distribution models for top-of-atmosphere radiative flux estimation from the Clouds and the Earth's Radiant Energy System instrument on the Terra satellite. Part I: Methodology. J. Ocean and Atmos. Tech., 22, 338–351.

[4] Loeb, N. G., N. Manalo-Smith, 2005, Top-of-atmosphere direct radiative effect of aerosols over global oceans from merged CERES and MODIS observations, J. Climate, 18, 3506–3526.

[5] Li Z., et al., 2007, Validation and understanding of Moderate Resolution Imaging Spectroradiometer aerosol products (C5) using ground-based measurements from the handheld Sun photometer network in China, J. Geophys. Res., 112, D22S07, doi:10.1029/2007JD008479.

[6] T. X.-P. Zhao, H. Yu, I. Laszlo, M. Chin, W. C. Conant, 2007, Derivation of component aerosol direct radiative forcing at the top of atmosphere for clear-sky oceans, JQSRT, 109/7, doi:10. 1016.

[7] Fu, Q., K.-N. Liou, 1993, Parameterization of the radiative properties of cirrus clouds. J. Atmos. Sci., 50, 2008–2025.

[8] Moody, E. G., M. D. King, S. Platnick, C.B. Schaaf, F. Gao, 2005, Spatially complete global spectral surface albedos: Value-added datasets derived from Terra MODIS land products. IEEE Trans. Geosci. and Rem. Sens., 43, 144–158.

[9] Streets, D. G., et al., 2003, An inventory of gaseous and primary aerosol emissions in Asia in the year 2000, J. Geophys Res., 108(D21), doi:10.1029/2002JD003093.

[10] Zhou, M., H. Yu, R. E. Dickinson, O. Dubovik, B. N. Holben, 2005, A normalized description of the direct effect of key aerosol types on solar radiation as estimated from Aerosol Robotic Network aerosols and Moderate Resolution Imaging Spectroradiometer albedos, J. Geophys. Res., doi:10.1029/2005JD005909.

[11] Huebert, B. J. et al., 2003, An overview of ACE-Asia: Strategies for quantifying the relationships between Asia aerosols and their climatic impacts. J. Geophys. Res., 108:8633, doi:10.1029/2003JD003550.

[12] Conant, B. C. et al., 2003, A model for the radiative forcing during ACE-Asia derived from CIRPAS Twin Otter and R/V Ronald H. Brown data and comparison with observations. J. Geophys. Res., 108:8661, doi:10.1029/2002JD003260.

[13] T. X.-P. Zhao, N. G. Loeb, I. Laszlo, Mi Zhou, 2008, Global component aerosol direct radiative effect at the top of atmosphere, J. Geophys. Res.,(submitted).

[14] Kinne, S., et al., 2006, An AeroCom initial assessment-optical properties in aerosol component modules of global models, Atmos. Chem. Phys., 6, 1815–1834.

[15] Textor. C., et al., 2006, Analysis and quantification of the diversities of aerosol life cycles within AeroCom, Atmos. Chem. Phys., 6, 5225–5246.

[16] Chin, M., P. Ginoux, S. Kinne, O. Torres, B. N. Holben, B. N. Duncan, R. V. Martin, J. A. Logan, A. Higurashi, T. Nakajima, T., 2002, Tropospheric aerosol optical thickness from the GOCART model and comparisons with satellite and sun photometer measurements, J. Atmos., Sci., 59, 461–483.

[17] Chin, M., D. A. Chu, R. Levy, L. A. Remer, Y. J. Kaufman, B. N. Holben, T. Eck, T., P. Ginoux, 2004, Aerosol distribution in the northern hemisphere during ACE-Asia: Results from global model, satellite observations, and sunphotometer measurements, J. Geophy. Res., 109, D23S90, doi:10.1029/2004JD004829.